Vaccine 37 (2019) 7256–7268

Contents lists available at ScienceDirect

Vaccine

journal homepage: www.elsevier.com/locate/vaccine

Therapy with multi-epitope virus-like particles of B19 parvovirus reduce tumor growth and lung metastasis in an aggressive breast cancer mouse model

Ángel de Jesús Jiménez-Chávez [a], Leticia Moreno-Fierros [a,*], Ismael Bustos-Jaimes [b]

[a] Biomedicine Unit, Faculty of Higher Studies Iztacala, National Autonomous University of Mexico, Avenida de los Barrios 1, Los Reyes Iztacala, Tlalnepantla 54090, Estado de México, Mexico
[b] Department of Biochemistry, Faculty of Medicine, National Autonomous University of Mexico (UNAM), Mexico City 04510, Mexico

ARTICLE INFO

Article history:
Received 2 March 2019
Received in revised form 26 August 2019
Accepted 20 September 2019
Available online 27 September 2019

Keywords:
Virus-like particles
Neoepitopes
Vaccine
Triple negative breast cancer

ABSTRACT

Triple-negative breast cancer is a major health problem that lacks molecular targets for therapy. Neoepitopes represent a viable option to induce antitumor immune responses, but they have limitations, such as low immunogenicity and tolerance induction. Parvovirus B19 virus-like particles may be used to deliver neoepitopes to prime cellular immunity. We designed and evaluated the therapeutic effect of VP2 B19-virus-like particles, with multi-neoepitopes, in a 4T1 breast cancer model. Balb/c mice received four therapeutic immunizations with multi-neoepitopes-virus-like, wild type-virus-like, vehicle, or virus-like plus Cry1Ac adjuvant particles, intraperitoneally and peritumorally. Tumor growth, lung macro-metastasis, and specific immune responses were evaluated. Therapeutic administration of multi-epitopes virus-like particles significantly delayed tumor growth and decreased the lung macro-metastasis number, in comparison to treatment with wild type-virus-like particles, which surprisingly also elicited antitumoral effects that were improved with the adjuvant. Only treatments with multi-epitope virus-like particles induced specific proliferative responses of CD8 and CD4 T lymphocytes and Granzyme-B production in lymphatic nodes local to the tumor. Treatment with recombinant multiple neoepitopes-virus-like particles induced specific cellular responses, inhibited tumor growth and macro-metastasis, thus B19-virus-like particles may function as an effective delivery system for neoepitopes for personalized immunotherapy.

1. Introduction

The incidence of breast cancer continues to increase, being the first cause of cancer death in women worldwide [1,2]. Particularly, triple-negative breast cancer (TNBC) is recognized for its aggressiveness, high recurrence rate, and few available treatments due to the lack of identified therapeutic molecular targets [3]. Because of these reasons, the personalized therapy approach might be beneficial for treating this type of cancer [4].

Personalized vaccines, using neoepitopes, have been shown to induce specific cellular immune responses to tumor cells, provoking tumor resection. Recently, the ability of this approach to increase progression-free survival and decrease metastasis was demonstrated in clinical trials [2,5]. In these and other reports, inducing specific cytotoxic CD8 T lymphocytes has been claimed as the main mechanism responsible of tumor elimination [6], although they also observed that Th1 CD4 cells participated in the establishment of an antitumor environment by releasing cytokines.

While the use of synthetic peptides as antigens for inducing immune responses to neoepitopes is used widely [7,8], it is not efficient, as it requires a large amount of the antigen to be administered and must be accompanied by adjuvants, which are frequently associated with toxic effects [9,10]. Moreover, to avoid antigen processing by non-professional antigen presenting cells, which may result in lymphocyte anergy or regulatory T cells

Abbreviations: VLP, virus-like particle; rMe-VLPs, recombinant multi-epitope virus-like particles; TNBC, triple negative breast cancer; MDSC, Myeloid-Derived Suppressor Cells.

* Corresponding author at: Laboratory 9, Biomedicine Unit, FES Iztacala, UNAM, Av. De los barrios 1, Los Reyes Iztacala, Tlalnepantla 54090, Estado de México, Mexico.
E-mail address: lemofi@unam.mx (L. Moreno-Fierros).

https://doi.org/10.1016/j.vaccine.2019.09.068
0264-410X/

[11,12], these antigens need to be applied directly into the nearby lymph nodes. So, to induce strong, long-lasting tumor specific immune responses, it is important to develop improved antigen delivery systems and effective, non-toxic adjuvants, which decrease the amount of antigen administered and favor antigen delivery to professional antigen presenting cells in local lymph nodes, for adequate processing and presentation of the antigen.

Multimeric compounds of viral structural proteins named virus-like particles (VLPs) are promising antigen delivery systems that are able to induce strong humoral and cellular responses towards coupled antigens [13,14]. VLPs are a subclass of viral nanoparticles which are spontaneously assembled from viral proteins in capsids that resemble virus morphology, they are biocompatible, biodegradable and are no infectious, thus multiple VLPs have been evaluated for their potential use in cancer immunotherapy [15–18]. Therefore, it is important to evaluate VLPs with additional desirable characteristics of purification, stability, and versatility. In this sense, proteins which allow the formation of chimeric VLPs are preferred because they may be able to carry several epitope-containing sequences. It is also important that additions to the chosen proteins do not affect their assembly properties and/or production yields.

In previous studies, B19-VLPs were proposed as a promising antigen delivery system due to their expression, purification, and assembly characteristics. The wild type VP2 protein (WT-VP2) protein of B19 can be produced on a large scale in *E. coli*, and this protein can be purified in a denatured state and renatured. Importantly, VLPs formed from the WT-VP2 protein can be assembled in capsids of approximately 20 nm, *in vitro*, in a cell-free environment [19]. Moreover, it has been reported that the WT-VP2 protein can be modified at its amino terminus to carry several sequences without affecting its production yields or its assembly properties [20]. Additionally, several parvovirus VLPs, with similar characteristics, have been shown to induce cellular responses through antigen cross-presentation by dendritic cells [21], indicating their potential use as antigen delivery systems.

In this work, we focused on the design of VLPs formed by the VP2 protein of the human parvovirus, B19, as a tumor antigen delivery system, and tested their therapeutic effects in a murine model of TNBC, induced using the aggressive, low immunogenic, and highly metastatic 4T1 tumor cell line. The neoepitopes (Tmtc2, Gprc5a, Qars) were selected from experimental studies of next generation sequencing of the 4T1 cell line [22,23], and we also included an epitope of survivin because of the role this protein plays in inhibiting apoptosis of tumor cells [24]. Although most of the identified neoepitopes in 4T1 cell line are recognized by CD4 T lymphocytes, we decided to choose neoepitopes recognized by CD8 T lymphocytes due their primary role in the direct elimination of tumor cells. The selected epitopes were coupled to the amino terminal region of the WT-VP2 protein of the parvovirus, as has been described for other chimeric VP2 proteins [25–27].

The recombinant VP2 multi-epitope vaccine assembled in VLPs (rMe-VLPs) was tested alone or with the adjuvant Cry1Ac protoxin, which is a delta-endotoxin from *Bacillus thuringiensis*. Cry1Ac protoxin was chosen because it has proven to be an effective systemic and mucosal adjuvant, able to improve the protection against diverse infection models, when it was used coadministered with antigens. Importantly when it was tested in a brucellosis mouse model Cry1Ac protoxin improved the cytotoxic responses [28], which are the kind of immune responses desired to achieve tumor immunity. Regarding the proposed adjuvant action mechanism of this protein it appears to rely in its capacity to activate antigen-presenting cells by upregulating the costimulatory molecules and inducing proinflammatory cytokines production [29].

2. Materials and Methods

2.1. Animals and cell line

Female, BALB/c mice, 6–8 weeks of age were used for this study. The mice were kept in micro-isolators, with sterile filter covers, had *ad libitum* access to water and food, and were housed under a dark/light period of 12:12 h in the FES Iztacala, UNAM. The animals were cared according to federal regulations (NOM-062-ZOO-1999, Ministry of Agriculture, Mexico). The immunization protocol was approved by the institutional animal care and use committee (IACUC).

4T1 mouse mammary carcinoma cells (ATCC, Manassas, Virginia, USA) were maintained for a limited time *in vitro* by passages in RPMI-1640 medium (Gibco®, Grand Island, New York, USA), containing penicillin (100 U/mL), streptomycin (100 μg/mL) and fungicide (0.75 μg/mL) (Sigma Aldrich, St. Luis, Misuri, USA) and supplemented with 10% FBS (Gibco®).

2.2. Design of B19 WT-VP2 chimeras

The expression vector of the WT-VP2 protein was previously constructed [19]. The sequences of the neoepitopes for CD8 responses Tmtc2 (QGVTVLAVSAVYDIFVFHRLKMKQILP), GPRC5a (FAICFSCLLAHALNLIKLVRGRKPLSW), and Qars (FPPDAINNF), which were previously identified by next generation sequencing of the 4T1 [22,23] cell line, and survivin tumor-associated antigen (GWEPDDNPI), were inserted in the amino terminal region of the WT-VP2 protein and separated from one another by three linkers with the sequence $A(EAAAK)_3A$. The DNA sequence was optimized for expression in *E. coli*, the recombinant multi-epitope-VP2 gene was chemically synthesized (Epoch Life Science Inc, Missouri, Texas, USA) in the pBSK vector and was subcloned to the expression vector pet22b (Novagen, Madison, Wisconsin, USA) between the NdeI and EcoRI sites. These constructs also encoded a tag of histidines at the carboxyl terminal end to facilitate purification. The final plasmids were called PETWT-VP2 and PET-rMe-VP2 who's codification for wild type VP2 and recombinant multi-epitope VP2 proteins respectively.

2.3. Expression and purification of B19V WT-VP2 and chimeras

Plasmids PETWT-VP2 and PET-rMe-VP2 were used to transform *E. coli* BL21 (DE3) cells (Novagen, Madison, Wisconsin, USA). The purification of WT-VP2, recombinant multi-epitope-VP2 (rMe-WT-VP2) proteins and GFP-WT-VP2 was based of the protocol previously reported for the purification of WT-VP2 protein with minor modifications [19,20]. Briefly, transformed bacteria were grown in LB medium (100 μg/mL) and induced to Abs600 = 0.6 with 0.1 mM of isopropyl β-D-thiogalactopyranoside (IPTG) for 16 h at 30 °C, in an orbital shaker to 200 rpm. The cells were harvested by centrifugation (5000g × 10 min) and the pellet was resuspended in lysis buffer (0.3 M NaCl, 50 mM sodium phosphate, pH 7). Cells were disrupted by ultrasonication and centrifuged at 5000g at 4 °C. The WT-VP2 and rMe-VP2 proteins remained in the insoluble fraction. To obtain the WT-VP2 proteins the pellets were washed with buffer A (0.3 M NaCl, 50 mM sodium phosphate, 2% Triton X-100, 3 M urea, pH 7), followed by buffer A containing 5 mM DTT, and finally, with lysis buffer. The remaining pellet was solubilized in column buffer (6 M guanidine hydrochloride (GuHCL), 0.3 M NaCl and 50 mM sodium phosphate, pH 6.3) and incubated for 24 h at 180 rpm and 37 °C. For the rMe-VP2 proteins, the pellets were solubilized in buffer A, and a change was made in the column buffer. The proteins were purified by immobilized metal affinity

chromatography (IMAC) under denaturing conditions, using a His-Pur Ni-NTA resin (Thermo, Waltham, Massachusetts, USA). Triton X-114 (0.1% v/v) was used in the wash buffer to eliminate Lipopolysaccharide excess [30]. The purified proteins were concentrated by filtration with 50 kDa centrifugation filters (Millipore, Burlington, Massachusetts, USA). Purity was assayed by SDS-PAGE analysis. The protein concentration was determined using the Bradford protein assay (Sigma Aldrich, st. Luis, Misuri, USA).

2.4. In vitro assembly of VLPs

VLPs were assembled by dialysis of 1.5 mL of purified WT-VP2 or rMe-VP2 protein (0.5 mg/mL) against 3×50 mL of PBS-arginine (0.2 M L-arginine, 137 mM NaCl, 2.7 mM KCl, 10 mM Na2HPO4, 1.8 mM KH2PO4, pH 7.4) at 4 °C for 36 h. After dialysis, the samples were filtered using a 0.22 μm filter and stored at 4 °C until use. The chimeric VLPs, composed of 100% rMe-VP2 protein (called rMe-VLPs), were able to assemble without the addition of WT-VP2. The correct assembly of WT-VLPs and rMe-VLPs was measured by dynamic light scattering using a Zetasizer μV (Malvern, Worcestershire, UK) equipped with a photodiode laser (830 nm). For each sample, 50 measurements were taken at 20 °C. The BALB/c mice were randomly separated into experimental groups (n = 5–8) and were immunized intraperitoneally and peritumoral as follows:

2.5. Therapeutic immunization

The tumors were induced by subcutaneous injection, into the sixth breast of BALB/c mice, of 3×10^3 4T1 cells that were freshly obtained from cell culture, with viability greater than 90% (evaluated by trypan blue exclusion). The BALB/c mice with palpable tumors were randomly separated into groups with 5–8 mice and each mice was simultaneously immunized intraperitoneally and s.c. peritumorally on days 7, 14, 21 and 28 post tumor induction with 50 μl of the vehicle (PBS), 50 μg of wild type VLPs (WT-VLPs) or 50 μg of recombinant multiepitope VLPs (rMe-VLPs) alone or plus 50 μg of adjuvant (protoxin Cry1Ac). Tumor growth was monitored with a digital caliper every 3 days and tumor volume was calculated according to the formula $V = L \times S^2/2$, where L is the longest side and S the shortest. On day 36 post-tumor induction, the animals were sacrificed using humane methods. The spleens, inguinal nodes, lungs, and the tumors were obtained for further analysis at indicated days.

It is important to mention that in this work, we used a lower number of 4T1 cells (3×10^3) to induce tumors in BALB/c mice. This cell concentration was chosen to avoid the induction of necrotic processes in the tumors observed when a higher concentration of cells was used. We wanted to avoid the induction of necrosis because it provokes painful tissue lesions in the animals, making it necessary to sacrifice the mice prematurely, and thus complicating the evaluation of the antitumor treatments.

2.6. Lung metastasis

For the analysis of the macro-metastases in the lungs, the same scheme described above was used. During sacrifice, the lungs were filled with 1 mL of a 10% India Ink solution (Winsor & Newton, London, UK), in PBS, through the trachea with the help of a cannula. The trachea was blocked by surgical thread and the lungs were extracted and washed 3 times with 10 mL of Fekete's solution (85 mL 70% ethanol, 10 mL 10% paraformaldehyde, and 5 mL acetic acid) and, the lungs were fixed in the same solution overnight. The macroscopic foci were counted and photographed with a stereoscopic microscope, OLYMPUS SZ CTV (Olympus, Tokyo, Japan). Metastatic index was calculated with the number of lung metastatic nodes/primary tumor weight.

2.7. Flow cytometry analysis

The spleen, inguinal lymph nodes and tumor of the different treatment groups were mechanically disintegrated through a plastic mesh, the cell suspension was filtered, and the red cells were lysed. The cells were washed and counted by Bio-Rad TC10™ automated cell counter (Hercules, California, USA). To characterize the populations, 1×10^6 cells were centrifuged at 400*g* for 5 min at 4 °C, and the pellet was treated with 1μg/mL of anti-CD16/32 antibody (Biolegend, San Diego, California, USA, cat# 101302), in 0.5% BSA-PBS to avoid non-specific binding of the antibodies. The cells were washed with BSA-PBS and incubated with the indicated combination of antibodies [CD3-APC, Granzyme-B–PE, CD11b-FITC (Biolegend, San Diego, California, USA, Cat#: 100236, 372207, 1012059)] or CD4-PeCy5, CD3-PeCy5, CD8-PE, Gr1-APC (ebioscience, San Diego, California, USA, Cat#: 150041, 150031, 120081, 108412) at an appropriate dilution for 30 min at 4 °C in the dark. Subsequently, the cells were washed to remove the excess antibody and fixed in 300 μl of 1% paraformaldehyde. T cell proliferation was assayed on the 15th day of treatment by labeling $3 \text{ X } 10^6$ inguinal node cells with CFSE (5 μM) (Molecular probes, Eugene, Oregon, USA, Cat#: 11524217), the cells were placed in 96-well plates and stimulated with 2 μg/mL of synthetic peptides or 20 μg/mL of rMe-VLPs for 5 days. Subsequently, the cells were recovered and stained for analysis as mentioned above. All data were acquired in a BD FACSCalibur Flow Cytometry System (RRID: SCR_000401) with the software BD CellQuest Pro (Franklin Lakes, New Jersey, USA, RRID: SCR_014489). The flow cytometry data were analyzed using the software Flowjo 7.6® (FlowJo, Ashland, Oregon, USA, RRID: SCR_008520).

2.8. Proliferation assay

T cell proliferation was assayed on the 15th day of treatment by labeling 3×10^6 inguinal node cells with CFSE (5 μM) (Molecular probes, Eugene, Oregon, USA, Cat#: 11524217), the cells were placed in 96-well plates and stimulated with 2 μg/mL of synthetic peptides or 20 μg/mL of rMe-VLPs for 5 days. Subsequently, the cells were recovered and stained for analysis as mentioned above.

2.9. Cytotoxicity assay

For the analysis of the cytotoxic effect of VLPs on 4T1 tumor cells, 3×10^4 4T1 cells were seeded in 96-well plates and stimulated with 25, 50, 100 or 200 μg/mL of WT-VLPs for 4 or 24 h. To analyze the cell viability to each cell well (100 μl), 10 μl of MTT (5 mg/mL) (Sigma Aldrich, st. Luis, Missouri, USA) was added and an additional 4 h were incubated, the formazan crystals were solubilized in acidified isopropanol and the absorbance was recorded at 570 nm. For the analysis of early, late apoptosis and necrosis, after incubation of the VLPs with the tumor cells as described above the cells were recovered and stained with Annexin V-APC (Biolegend, San Diego, California, USA, cat # 640920) and propidium iodide (Sigma Aldrich, st. Luis, Missouri, USA) and analyzed by flow cytometry with a FACSCalibur cytometer, in which 10,000 events, per sample, were obtained.

The analysis of cell cytotoxicity mediated by T cells was assayed on the 15th day post immunization, non-adherent cells from the inguinal node were used to isolated T lymphocytes by negative selection with MACS CD19 microbeads (Miltenyi Biotec, Bergisch, Germany, cat no 130-121-301), T cells were counted and co-cultured with 3×10^4 4T1 cells stained with CFSE for 4 h. Cells

were recovered, stained with Annexin V-APC and analyzed by flow cytometry with a FACSCalibur cytometer, in which 20,000 events, per sample, were obtained.

2.10. Statistical analysis

All the data obtained was analyzed with the Graphpad Prism software (RRID: SCR_002798), one way analysis of variance (ANOVA) and *t* test were used to determine significant differences between the groups, which were indicated when the *p*-value was ≤0.1, ≤0.05, ≤0.01 or ≤0.001 and were marked as *, **, *** or ****, respectively. The results are shown as mean ± standard deviation (SD) or standard error mean (SEM), as indicated.

3. Results

3.1. Design and production of recombinant proteins

The process used to construct WT-VP2 and GFP-WT-VP2 were the same process used in previous works [19,20], while the rMe-VP2 construction was analyzed *in silico*, with the objective of determining the secondary and tertiary structure of the multi-epitope region. Several arrangements of the epitopes were tested, and the predicted arrangement, with alpha helix-forming linkers and linear epitopes, was selected because this arrangement increased the solubility of the protein, which facilitated its assembly into VLPs (data not shown).

The rMe-VP2 construction (Fig. 1A) was conformed by the WT-VP2 plus the neoepitopes, Tmtc2, Gprc5a, and Qars, which were identified by next generation sequencing of the 4T1 cell line as epitopes recognized by CD8 cells [22,23], and the tumor associated antigen (TAA) survivin 66–74 epitope, which has been reported to induce tumor immunity in the spontaneously metastasizing 4T1 breast cancer model [31]. WT-VP2, GFP-WT-VP2 and rMe-VP2 were overexpressed in *E. coli* BL21 (DE3) cells as inclusion bodies, and subsequently, the proteins were purified under denaturing conditions, previously reported [19].

The WT-VP2 and GFP-WT-VP2 protein was purified with the previously reported protocol [19,20], with minor modifications, and was stored in elution buffer until its assembly (Fig. 1B). The rMe-VP2 protein showed slight changes in solubility, since a significant percentage of the protein was solubilized in the inclusion bodies wash buffer, unlike the WT-VP2 protein which does not solubilize in this buffer. As a result, we washed the pellets with washing buffer that did not contain urea, and then added 5 M GuHCL to the rMe-VP2 protein to solubilize it, to be then purified by Immobilized Metal Affinity Chromatography (IMAC) (Fig. 1B). This modification was performed because a concentration of 3 M GuHCL did not permit purification of the protein with IMAC. This phenomenon has already been reported for other WT-VP2 protein chimeras [20] and is possibly due to incomplete denaturation, which allows the formation of tertiary structures that block the exposure of the histidine tag. The increased concentration of this chaotropic agent resolved the problem and allowed rMe-VP2 proteins to be purified by IMAC.

The adjuvant recombinant Cry1Ac protoxin was produced and purified according to previous works without modifications and was kept at 4 °C until its use [32].

3.2. Assembly of VLPs

The assembly of VLPs with the WT-VP2 protein produced capsids 22–24 nm in diameter that coincided with reports for this

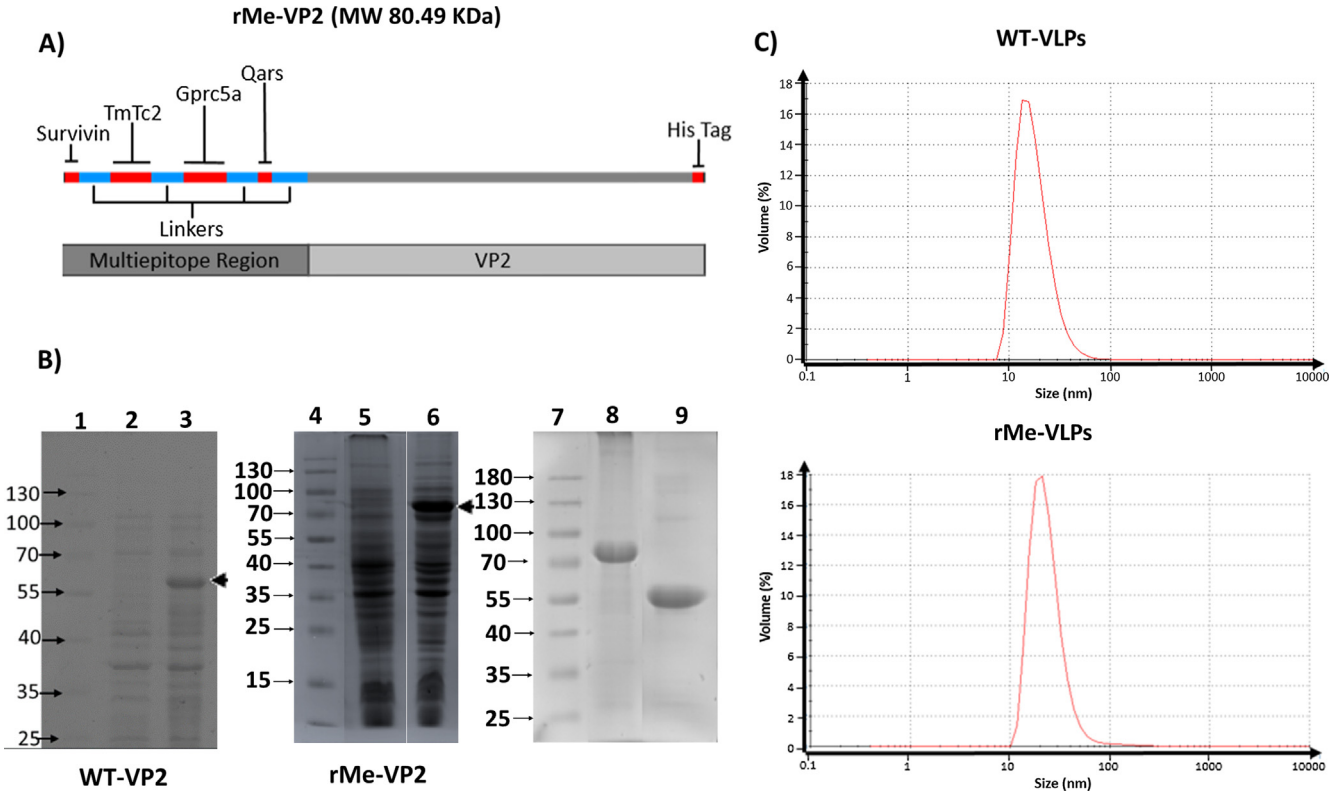

Fig. 1. Protein expression and assembly of VLPs. (A) Composition of chimeric multi-epitope construction of rMe-VP2. (B) Overexpression of WT-VP2 and rMe-VP2 proteins, following IPTG-induction for 18 h at 30 °C in BL21DE3 *E. coli* cells. Proteins from non-induced (2,5) and induced cells (3,6). The MW markers are represented by (1,4,7). The ~60 and ~80 kDa bands, corresponding to the expected MW for WT-VP2 and rMe-VP2, respectively, are marked with black arrow heads at 3 and 6. WT-VP2 (9) and rMe-VP2 (8) purified by IMAC. (C) Size results of the VLPs, acquired using dynamic light scattering. VLPs were assembled as indicated in Materials and Methods by dialysis of pure proteins against of PBS + 0.2 M arginine. 50 measurements were completed for each sample and peaks of ~20 nm were observed in both WT- and rMe-VLPs.

protein [19]. The rMe-VP2 protein was assembled alone or by adding different radii of the WT-VP2 protein (data not shown). In all cases, VLPs that coincided with the reported size of the WT-VLPs were observed. Consequently, we decided to work only with capsids formed by 100% of the rMe-VP2 protein, to ensure the presence of the multi-epitope fraction in the assembled capsids. The assembly with 100% chimeric VP2 was also recently reported [20]. The assembly of the rMe-VLPs produced monodisperse species of 20 ± 3.0 nm in diameter (Fig. 1C).

3.3. Antitumor effect of VLPs in mice

To test the possible antitumor effect of the rMe-VLPs in established tumors, mice were implanted with 4T1 cells and then immunized with rMe-VLPs with or without the adjuvant or with WT-VLPs as a control. 50 μg of each protein in the form of VLPs, was administered intraperitoneally and peritumorally simultaneously every 7 days during the experiments. Unexpectedly, we observed a delay in tumor growth in mice treated with WT-VLPs and WT-VLPs + adjuvant, with no differences between treatment with WT-VLPs with or without the adjuvant (Fig. 2A). Tumor growth in these groups was significantly lower than that observed in mice treated with the PBS vehicle. Mice immunized with rMe-VLPs, with and without adjuvant showed a significant delay in tumor growth compared to mice treated with the vehicle and significantly less tumor growth than mice treated with WT-VLPs (Fig. 2A, B). Treatments with rMe-VLPs with the adjuvant showed the smallest tumor sizes until day 36, even then exhibiting non-measurable tumors in 4/7 mice. The tumors excised on day 36 showed large volume with similar measurements in groups PBS and WT-VLPs, however due to their irregular shape the large sides of these tumors were not precisely measurable *in vivo*, so the volumes of excised tumors were higher (Fig. 2C). The addition of the adjuvant partially improved the response observed from treatment with WT-VLPs and rMe-VLPs in excised tumors, although not significantly.

3.4. Inhibition of macro-metastasis in the lung

Due to the importance of metastasis in cancer mortality, we decided to evaluate the effect of our treatment on the establishment of lung metastasis. For this evaluation, we injected 1×10^4 or 3×10^3 4T1 cells, subcutaneously, in the 6th breast of BALB/c mice. The treatments were applied as mentioned in the Materials and Methods. On day 32, the lungs of the mice were stained with 10% Indian ink to allow visualization of the metastatic nodules. Our results showed that treatment with rMe-VLPs significantly reduced the metastatic index and the number and size of

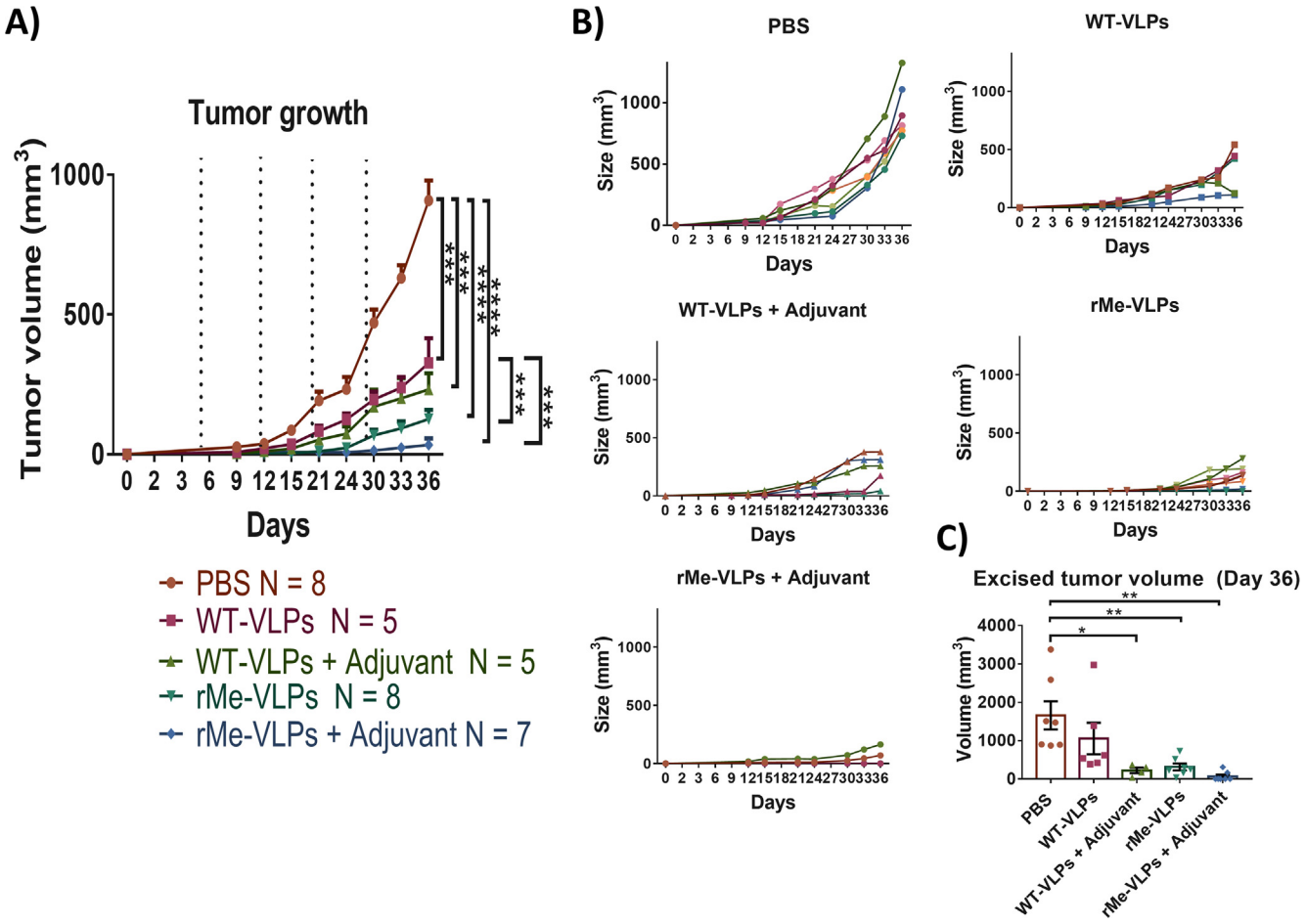

Fig. 2. rMe-VLPs treatment reduced tumor growth in BALB/c mice subcutaneously inoculated with 4T1 cells. Female BALB/c mice were subcutaneously injected in the sixth breast with 3×10^3 4T1 cells and treatments were applied on the indicated days (dotted lines) by peritumoral and intraperitoneal routes as detailed in Materials and Methods. Tumor growth was monitored every third day. The tumor size was measured with a digital caliper and the volume was calculated with the formula $V = (L \times S^2)/2$. (A) Graphs represent the mean ± SEM of tumor size volumes recorded following the distinct treatments with PBS, WT-VLPs, WT-VLPs + adjuvant, rMe-VLPs, and rMe-VLPs + adjuvant. (B) Graphs show tumor volume sizes recorded for individual mice within each treatment. (C) Mean volume size of tumors excised and recorded at day 36, following the distinct treatments. The data is represented as mean ± SEM. N = 5–8. *, **, ***, ****denote significant differences, where the *p*-value was ≤0.1, 0.05, 0.01 or 0.001, respectively.

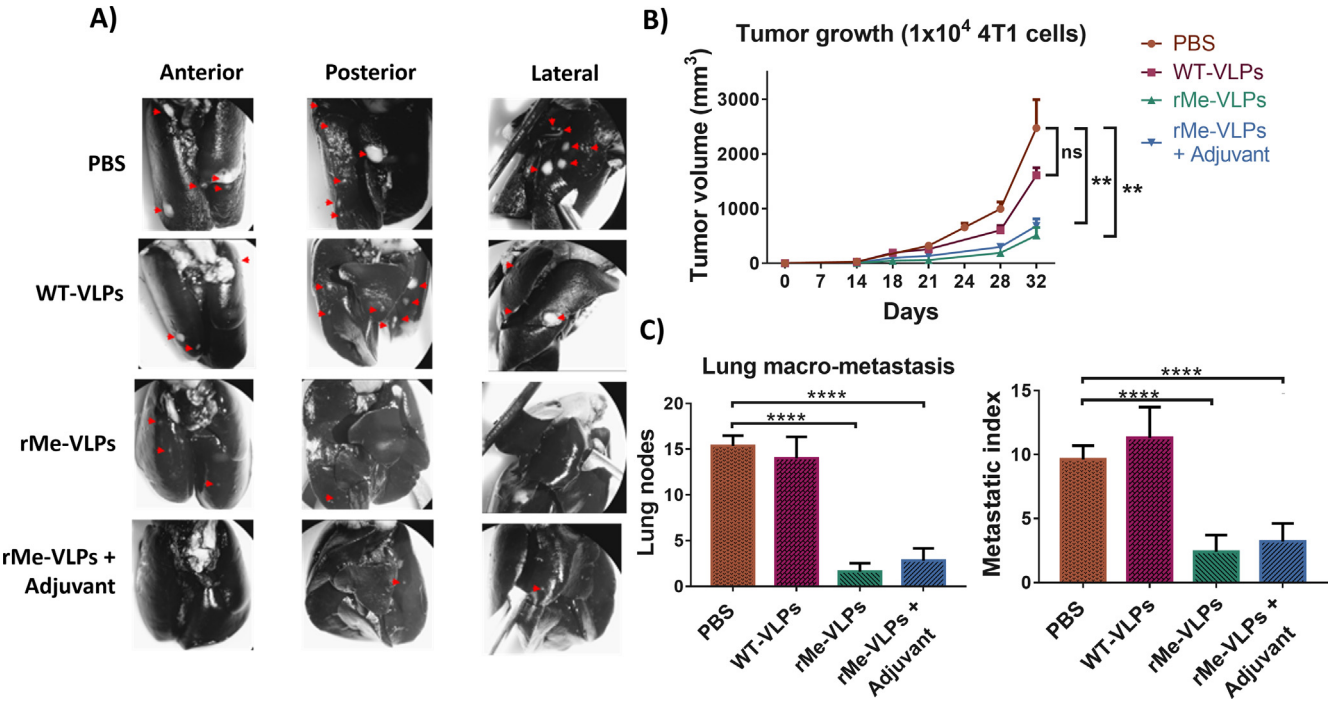

Fig. 3. rMe-VLPs treatment reduced lung macro-metastasis induced by 1×10^4 cells 4T1. (A) Tumor-bearing mice received treatments as mentioned in Materials and Methods. At day 32, the mice were euthanized and the lungs were filled with 10% India ink solution through a tracheotomy. The lungs were extracted, washed, fixed, and photographed with a stereoscopic microscope. The anterior, posterior, and lateral views are shown, where the arrowheads indicate metastatic nodes. (B) Temporal course of tumor growth recorded after subcutaneous injection of 1×10^4 cells 4T1 in mice that received the indicated treatments every 7 days by intraperitoneal and peritumoral routes. (C) The number of metastatic nodes recorded in the lungs of each mouse. The data is represented as mean ± SEM. N = 6. **, ***denote significant differences, where the *p*-value was ≤0.05 or 0.01, respectively.

macro-metastases induced by 1×10^4 cells or 3×10^3 4T1 cells (Fig. 3A, S1), while WT-VLPs did not have any effect on rate of metastasis. Tumor growth by injection of 1×10^4 4T1 cells in mice showed a behavior like that observed with the injection of 3×10^3 4T1 cells (Fig. 3B), except WT-VLPs did not have a significant effect in tumor growth.

Supplementary data associated with this article can be found, in the online version, at https://doi.org/10.1016/j.vaccine.2019.09.068.

The number of metastases by injection of 3×10^3 4T1 cells in the PBS group was higher than that observed by the injection of 1×10^4 4T1 cells (Fig. S1). The treatment of mice with rMe-VLPs, with and without the adjuvant, decreased the amount and size of metastatic nodules in the lungs in comparison to the mice treated with the vehicle or with the WT-VLPs (Fig. 3C). There were no differences between mice treated with rMe-VLPs and rMe-VLPs + adjuvant.

3.5. Characterization of populations of T lymphocytes and MDSC

To determine if the immune populations were modified by the treatments, the populations present in the spleen and in the tumor of the treated and untreated mice were analyzed by flow cytometry. We observed that the proportions of $CD3^+CD4^+$ cells and $CD3^+$-$CD8^+$ T lymphocytes decreased in their percentages in the mice treated with the vehicle, and this decrease was significantly lower than the values found in healthy mice without tumors (Fig. 4A, B). The treatments with WT-VLPs and rMe-VLPs partially re-established the values of these populations, however, only rMe-VLPs with and without the adjuvant were significantly different from the vehicle group (Fig. 4B). To analyze the Myeloid-Derived Suppressor Cells (MDSC), we use CD11b and Gr1 markers, as these two markers are known to delimit the suppressor population in this model, as previously reported [33,34]. We found a significant increase of this population in mice treated with the vehicle, with respect to healthy mice (Fig. 4C). Regarding the treatments, we observed that WT-VLPs + adjuvant and rMe-VLPs + adjuvant decreased this population in the spleen, while in the tumor, all treatments decreased the proportion of these cells, with a significantly lower proportion observed only after treatment with WT-VLPs + adjuvant (Fig. 4D). Importantly, these results show that the Cry1Ac protoxin as adjuvant has an inhibitory effect on the MDSC population, which deserves further characterization.

3.6. Proliferation and cytotoxicity of T lymphocytes

Proliferation assays were performed, by tracing the loss of fluorescent compound Carboxyfluorescein succinimidyl ester (CFSE), to determine if the treatments were able to induce specific cellular responses towards the tumor. On day 15 of treatment, the animals were sacrificed, and the spleen and inguinal node cells were stained with CFSE. The cells were seeded and stimulated for 5 days using a pool of peptides of neoepitopes or rMe-VLPs as stimuli or WT-VLPs/unrelated peptides as control (Fig. S2). The analysis showed a significant increase in proliferation of lymphocytes CD4 in mice treated with rMe-VLPs, with and without the adjuvant, after the *in vitro* stimulation with the peptides or rMe-VLPs. These results showed that rMe-VLPs were able to induce CD4 specific responses in inguinal nodes (Fig. 5B). The proliferative responses of lymphocytes CD8 were similar to those of CD4, but the proliferation was observed only after the stimulus with peptides or rMe-VLPs (Fig. 5E). Mice treated with WT-VLPs only exhibited proliferation towards WT-VLPs stimulus (Fig. S2). No differences were observed with the adjuvant addition. To prove that CD8 lymphocytes had a cytotoxic profile, we determined the production of Granzyme-B. Results showed a significant increase in the

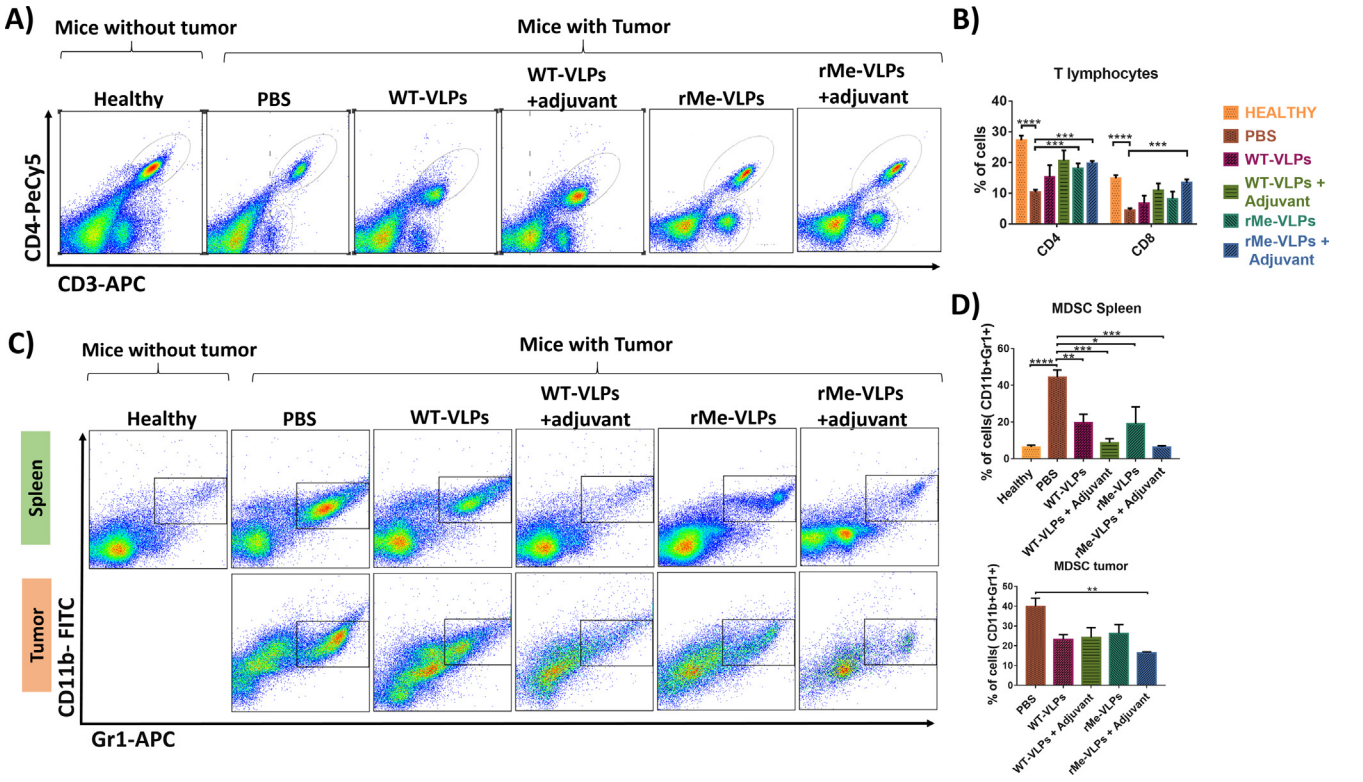

Fig. 4. Treatments with VLPs provoked a minor reduction of T lymphocytes and a lower percentage of MDSC in the spleen and tumor. BALB/c mice treated as indicated in Fig. 2 were euthanized at 36 days post tumor induction. The spleen and tumor were extirpated and disaggregated. (A) Representative dot plots indicating the proportion of T lymphocytes in the spleens of healthy vs tumor induced mice using CD3+ and CD4+ markers. The population CD3+CD4− was used to estimate the proportion of CD8 lymphocytes. (B) Analysis of the proportion of CD3+CD4+ and CD3+CD8+ lymphocytes in the spleen. (C) Representative dot plots indicating CD11b+Gr1+ MDSC populations in spleen or tumor which were used for the analysis shown in D, are shown in the rectangle regions. Data was acquired with a FACSCalibur cytometer and 50,000 events were acquired. (D) Proportions of MDSC in spleen or tumor, the data in bar graphs is represented as mean ± SEM. N = 6. *, **, ***, ****denote significant differences, where the *p*-value was ≤0.1, 0.05, 0.01 or 0.001, respectively.

percentage of CD8 + Granzyme-B + cells after stimulus with the peptides or rMe-VLPs in mice treated with rMe-VLPs alone or with the adjuvant (Fig. 6B). Furthermore the cytotoxicity on 4T1 cells of CD8 T lymphocytes isolated from immunized mice, was also evaluated *in vitro,* increased apoptosis evaluated by the expression of anexin-V in CFSE stained 4T1 cells was induced by cells from rMe-VLPs immunized mice in comparison with lymphocytes unimmunized, further confirming the induction of specific cytotoxic responses (Fig. 6E).

4. Effect of WT-VLPs on 4T1 tumor cells

Due to the unexpected effect of WT-VLPs on tumor growth, it was evaluated whether they were able to enter the tumor after peritumoral administration, the results showed that GFP-VLPs [20] can enter the tumor after 1 h administration and can be detected even 24 h after administration (Fig. 7A). In-cell western analysis showed that VLPs can bind to 4T1 cells after 1 h of incubation (Fig. 7B). It was observed that WT-VLPs can induce high antibody titers in serum from immunized mice (Fig. 7C), these antibodies show low binding to 4 T1 cells (Fig. 7B right) in comparison with the binding of VLPs. The evaluation of the effects of this union of the WT-VLPs to the tumor cells showed that can lead to the blockage of the union of the 4T1 cells to a fibronectin matrix (Fig. 7D) and can affect their migration (Fig. 7E). Besides, after 24 h of stimulation with WT-VLPs, an increase in the percentage of tumor cells in early (Fig. 7F, G left) and late apoptosis (Fig. 7G right) was observed, in addition to a decrease in cell metabolism measured by the reduction of MTT to formazan crystals (Fig. 7H), it was not observed that VLPs induce early apoptosis in primary culture lymphocytes at any of the concentrations evaluated (Fig. S3). Altogether these results indicating WT-VLPs can bind to 4T1 cells and induce apoptosis suggest direct effects on tumor cells which help to explain the antitumor effects observed.

5. Discussion

Currently, immunotherapy has been restricted to cancers with recognized molecular targets. Therefore, cancers, such as TNBC, continue to be cancers with little expectation of a cure and limited, available treatment options. As a result, these cancers without recognized molecular targets continue to be treated with chemotherapy and radiotherapy. The use of neoepitopes represents an alternative to provide specific targets in tumors that lack recognized molecular targets. However, to improve the ability of neoepitopes to induce antitumor immunity, it is still necessary to develop appropriate antigen delivery systems.

The results of this study support the use of VLPs, formed by the VP2 protein of the human parvovirus B19, as a promising tumor antigen delivery system, with the potential therapeutic effect as it functions in a murine a model of triple-negative breast cancer. Coinciding with previous reports, our present results showed that additions of epitope sequences at the amino terminal region of WT-VP2 does not alter its assembly properties [20,27], further supporting the advantage of this VLP system to be used as antigen delivery system.

We found that intraperitoneal and peritumoral administration of rMe-VLPs, loaded with multiple neoepitopes (Gprc5a, Tmtc2,

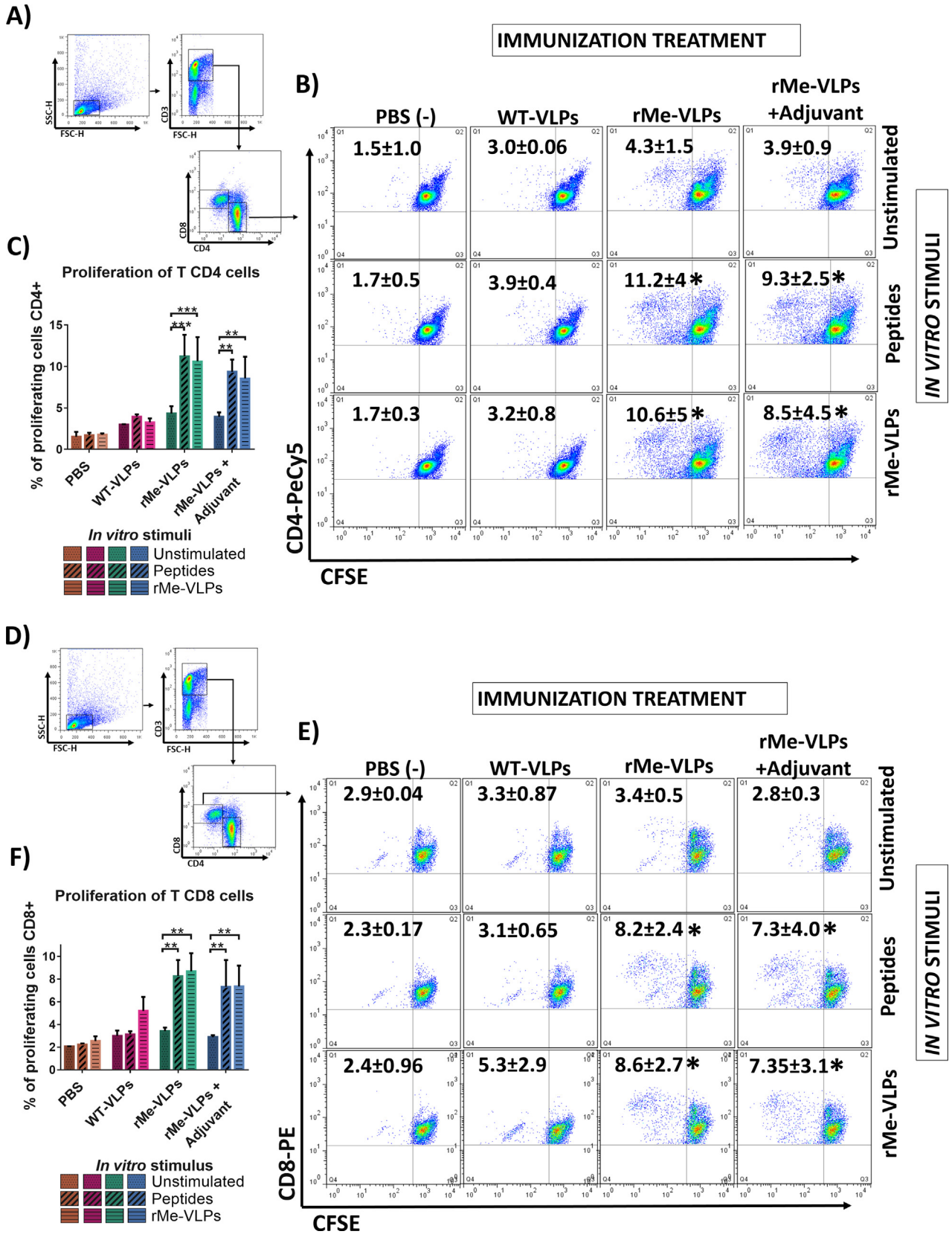

Fig. 5. rMe-VLPs treatment induced specific T CD4 and T CD8 proliferative responses in the inguinal node. Mice were injected subcutaneously with 3×10^3 4T1 cells and received a single immunization at day 7 with any of the indicated treatments. The mice were sacrificed on day 15 of the study. Inguinal lymph nodes were removed and disaggregated. 3×10^6 cells were stained with CFSE as is described in the Materials and Methods section. The cells were stimulated with peptides (2 μg/mL) or with rMe-VLPs (20 μg/mL) for five days. Cells were recovered, stained with anti CD3, CD4 and CD8 antibodies, and analyzed by flow cytometry with a FACSCalibur cytometer, in which 50,000 events, per sample, were obtained. (A), (D) Flow cytometry gating strategy, the figure shows the regions used to isolated CD4 and CD8 cells for the proliferation analysis shown in B and E. Representative dot plot of proliferation of CD3+CD4+ (B) and CD3+CD8+ (E) gated cells, mean ± SD are shown. (C), (F) The data in bar graphs is represented as mean ± SEM. N = 3. **, *** denote significant differences, where the p-value was ≤0.05 or 0.01, respectively.

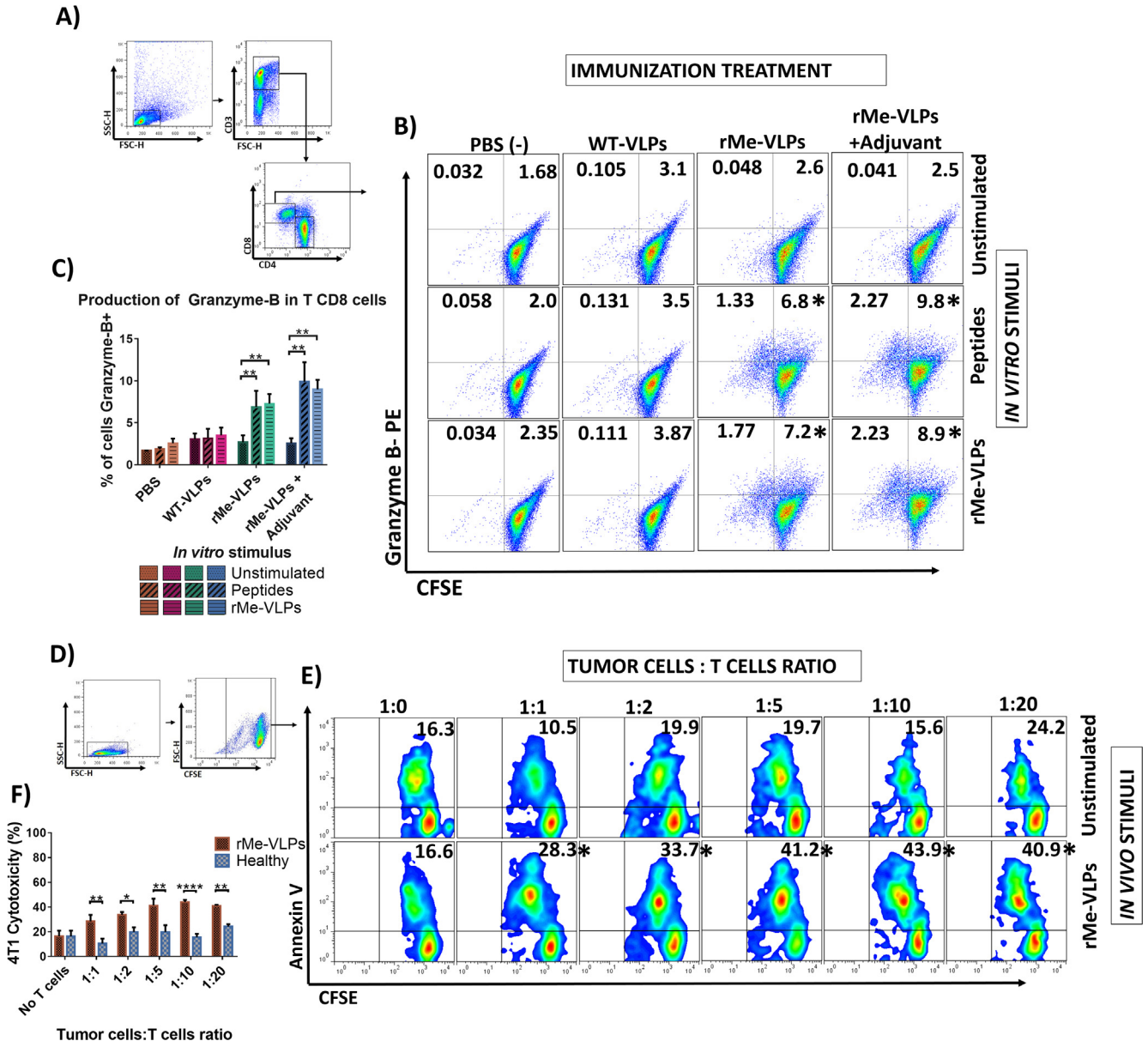

Fig. 6. rMe-VLPs treatment induces Granzima-B production in T CD8 cells and induce cytotoxicity of tumor cells mediated by T cells of inguinal node. Mice were injected subcutaneously with 1×10^4 4T1 cells and received a single immunization at day 7 with any of the indicated treatments. The mice were sacrificed on day 15 of the study. Inguinal lymph nodes were removed and disaggregated. 3×10^6 cells were stained with CFSE as described in the Materials and Methods section. The cells were stimulated with peptides (2 μg/mL) or with rMe-VLPs (20 μg/mL) for five days. Cells were recovered, stained with anti CD3-PeCy5 and anti CD8-APC, anti Granzyme-B -PE antibodies, and analyzed by flow cytometry with a FACSCalibur cytometer, in which 50,000 events, per sample, were obtained. (A) Flow cytometry gating strategy, the figure shows the regions used to isolated CD8 cells for the analysis shown in B. (B) Representative dot plots of CD8 gated cells are shown, mean of the quadrants are shown. (C) The data in bar graphs is represented as mean ± SEM. For the analysis of cell cytotoxicity mediated by T cells, the mice were immunized as described in the materials and methods section, the inguinal node T lymphocytes were isolated by negative selection with magnetic beads and were co-cultured with 4T1-CFSE cells for 4 h. Cells were recovered, stained with Annexin V-APC and analyzed by flow cytometry with a FACSCalibur cytometer, in which 20,000 events, per sample, were obtained. (D) Flow cytometry gating strategy, the figure shows the regions used to isolated 4T1- CFSE+ cells for the analysis shown in E. (E) Representative dot plots of 4T1- CFSE+ cells positives to Annexin V, mean of the quadrants are shown. (F) % of cytotoxicity of 4T1 cells, the data in bar graphs is represented as mean ± SEM. N = 3. *, **, ****denote significant differences, where the p-value was ≤0.1, 0.05 or 0.001 respectively.

Qars) and a TAA (survivin), are able to significantly delay tumor growth induced by the s.c. injection of 1×10^4 or 3×10^3 4T1 cells, where 4/7 mice reached complete tumor remission after the co-administration of rMe-VLPs with the adjuvant, Cry1Ac protoxin. Despite this result, total remission was only attained when tumors were induced with the lower dose of 3×10^3 4T1 cells. However, it is important to point out that a significant delay in tumor growth was observed, with both concentrations of cancer cells, at the end of the study.

Immunization with rMe-VLPs also significantly reduced the size and number of nodules of macro-metastases in the lungs, which was induced by s.c administration of both concentrations of 4T1 cells, rMe-VLPs group also showed lower metastatic index than WT-VLPs and PBS groups, therefore, the decrease in the size of the main tumor induced by rMe-VLPs may be related to a lower metastatic seeding in the lung. Moreover, our results are similar to a previous report that showed a lower concentration of 4T1 cells induced a greater number of macro-metastasis in the lungs of untreated mice [35].

Due to their small size of approximately 20 nm, B19-VLPs may be capable of directly entering lymph nodes local to the tumor, in a similar way that has been reported for porcine parvovirus VLPs,

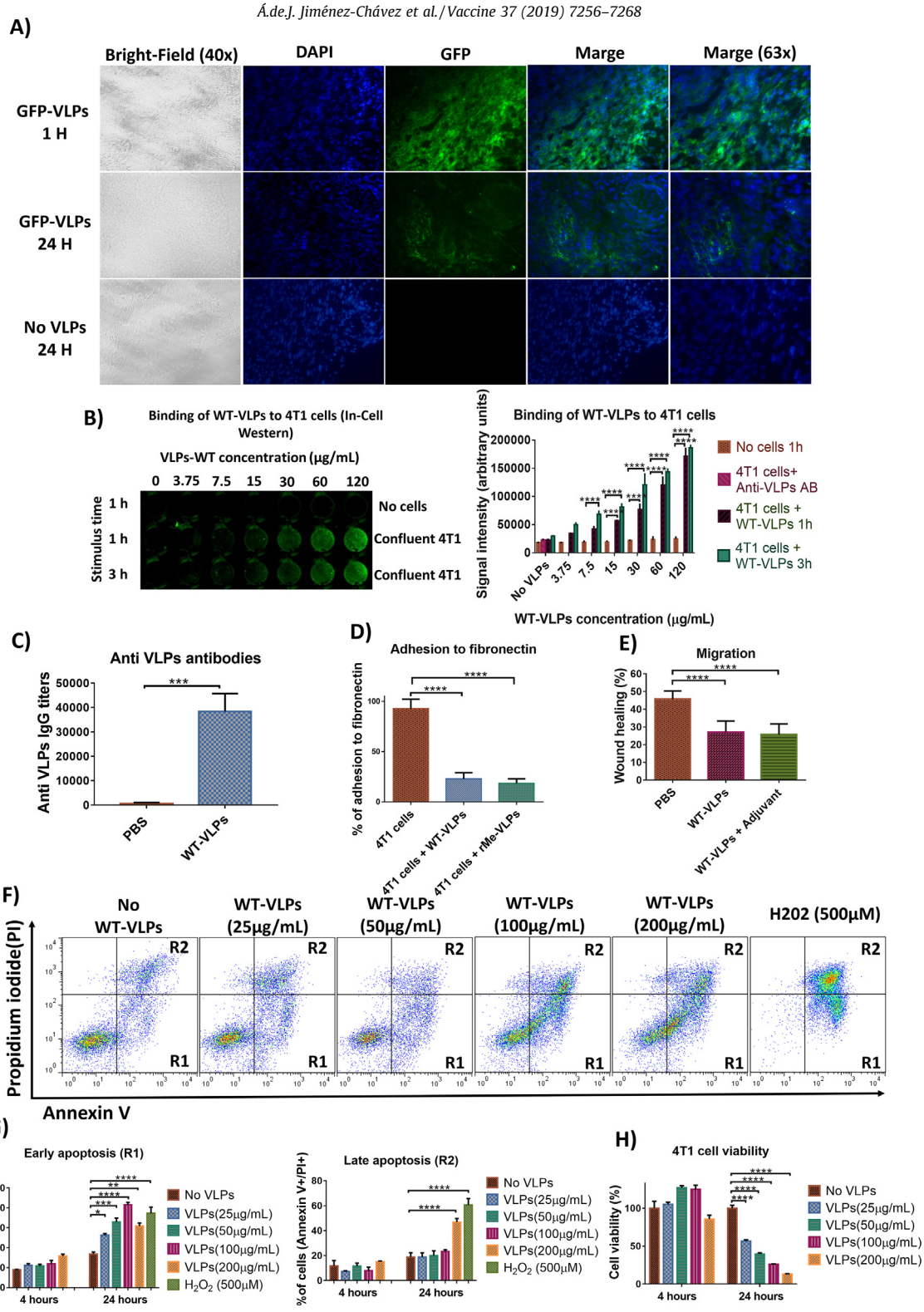

Fig. 7. WT-VLPs can entry to tumor, bound to 4T1 cells and affected migration, adhesion to fibronectin and induce apoptosis. (A) Entry of GFP-VLPS into tumors, 50 µg of GFP-VLPs were injected s.c. Near the breast and the primary tumor was removed after 1 and 24 h, 5 µm cuts were made, the nuclei were stained with DAPI and photographs (40×) were taken with a Leica fluorescence microscope. (B) Binding of VLPs to tumor cells, 4T1 cells were stimulated with increasing concentrations of WT-VLPs, for 1 and 3 h. The wells were washed and polyclonal antibody, anti-WT-VLPs, was used to detect VLPs binding to 4T1 cells (left), secondary Dye 800 anti-rabbit monoclonal antibody was used. Signal intensity was determined with an Oddissey LICOR scanner, right panel shown analysis of signal intensity. (C) Anti-VLPs antibody titers induced after 3 weekly immunizations with WT-VLPs. (D) In vitro adhesion of 4T1 cells to fibronectin. 96-well plates were covered with fibronectin (20 µg/well) and 1×10^5 4 T1 non-adherent cells were incubated with 50 µg/mL of WT-VLPs or rMe-VLPs for 30 min, at room temperature. The cells were added to the wells and incubated for 2 h. Crystal violet was used to determinate adhered cells. (E) Percentage of migration, Wound healing assay of 4T1, confluent monolayer was scratched with a yellow tip and cultured for 24 h. PBS, WT-VLPs (50 µg/mL) alone or with adjuvant (50 µg/mL) were used as a stimulus and wound healing was calculate with ImageJ software. (F) Dot plots representative of the induction of early apoptosis (Annexin V+, R1), late apoptosis (Annexin V+PI+, R2) and necrosis (PI+) in 4T1 cells induced by different concentrations of WT-VLPs after 24 h of stimulation. (G) Analysis of the induction of early (left) or late (right) apoptosis of 4T1 cells after 4 or 24 h of stimulation with different concentrations of WT-VLPs. (H) Analysis of the cell viability of 4T1 cells stimulated with different concentrations of WT-VLPs by reducing MTT after 4 or 24 h of stimulation. The data is represented as mean ± SEM. N = 6. *, **, ***, **** denotes significant differences, where the p-value was ≤0.1, 0.05, 0.01 or 0.001 respectively. (For interpretation of the references to color in this figure legend, the reader is referred to the web version of this article.)

which were captured in lymph nodes, processed by CD8 + CD11b + dendritic cells, and presented to T lymphocytes [21,36–38]. Although the neoepitopes contained in rMe-VLPs were chosen as CD8 epitopes, searching for the induction cytotoxic of immune responses; due to their size (more than 9 a.a.), they are also capable of functioning as CD4 epitopes. Likewise, most of the neoepitopes identified in the 4T1 cell line, by Kreiter et al were recognized by CD4 cells [22]. Moreover, due to the exogenous nature of VLPs, a presentation in MHC II is also possible, thus the induction of both types of cellular responses, in the inguinal lymph nodes induced in present study by the immunization with rMe-VLPs containing CD8 epitopes, was expected to occur, and may also be contributing to favor the induction of effective antitumor responses. Indeed the induction of CD4 Th1 responses also has been shown to play an important role in the induction of strong antitumor responses [39,40]. Our results also indicate that rMe-VLPs can be captured, processed, and presented to CD4 and CD8 T lymphocytes at the inguinal lymph nodes.

In addition, an increase in the proportion of CD8 T lymphocytes producing Granzyme-B was also observed in inguinal nodes, moreover when cytotoxicity on 4T1 cells of CD8 T lymphocytes was evaluated *in vitro* increased apoptosis was induced by cells from rMe-VLPs immunized mice. These results suggest that immunization with rMe-VLPs can induce specific cytotoxic T lymphocyte responses to neoepitopes. The induction of specific immune responses to tumor antigens in nearby lymph nodes has been reported to be important since these sites are the first to be invaded during the early phase of metastasis [41,42]. Therefore, the induction of cellular responses at this site may be related to the decrease in the observed metastatic rate.

Although in present study we focused in the characterization of the cellular immune response and the antibody response was not analyzed, because the CD8 epitopes used contained non exposed domains, the contribution of antibody responses in the antitumor effects induced by immunization with WT-VLP and rMe-VLP, rest to be determined. Despite anti VLPs antibodies did not show significant binding to 4T1 cells (Fig. 7B right) VLPs are immunogenic, as induce significant antibody titers (Fig. 7C), so the induction of ADCC in the presence of VLPs, which can bind to tumor cells might occur.

In addition to the induction of cellular responses at the local level, we also observed changes in cell populations of the spleen. Mice immunized with WT-VLPs and rMe-VLPs maintained the proportion of CD4 and CD8 T lymphocytes at normal levels in the spleen, animals treated with PBS only displayed a significant decrease of these cell populations in the spleen [43]. This decrease in lymphocyte proportions has been associated with the increase of suppressor populations in this organ that can lead to anergy and lymphocyte apoptosis [44]. So, we also analyzed the MDSC proportion, which has been reported as the main suppressor cell in the 4T1 model [45]. Our results showed that PBS treated mice presented a significant increase in the CD11b + Gr1 + population that denotes the MDSC in the spleen, while the mice immunized with WT-VLPs or rMe-VLPs with and without adjuvant showed a significant decrease of these cells, with a greater decrease with the addition of the adjuvant with respect to the PBS group. These results suggest that the adjuvant, protoxin Cry1Ac, may have some effect in decreasing this MDSC population, this finding is quite relevant due to the role of this population in tumor progression, this effect could be related with the capacity of Cry1Ac protoxin to induce the differentiation of these cells, as has been described by diverse adjuvants, particularly by agonists targeting TLRs 7/8 or 9 [46], but this possibility remains to be determined. The adjuvant mechanism of Cry1Ac protoxin is related with the capacity to activate antigen presenting cells by activating MAPK pathways [29]. Another possibility of the effect of Cry1Ac might be the induction of apoptosis in MDSC, but this deserves further investigation.

WT-VLPs showed an unexpected effect on tumor growth induced with 1×10^3 4T1 cells. A lower median size was observed in WT-VLPs and WT-VLPs plus adjuvant, these VLPs also show effects in MDSC population in the spleen, suggesting that they may have an antitumoral effect not mediated by specific cellular immune responses. Some reports have shown that VLPs formed by the WT-VP2 protein of parvovirus B19 are able to bind to the Gb4 globoside and $\alpha5\beta1$ integrin [47,48], both of which have been related to the induction of proliferation in tumor cells, through the activation of signaling pathways such as MAPK [49–51]. In this study, we observed that VLPs can access into tumors and stay there at least 24 h after injection, this may be due to the effect of enhancing permeability and retention of particles described in tumors [51]. We performed some assays to determine whether WT-VLPs may bind to or affect some 4T1 functions. We observed that WT-VLPs could bind directly to 4T1 cells, *in vitro*, and affected their migration and binding to fibronectin (ligand of $\alpha5\beta1$ integrin). In addition, the VLPs were able to induce apoptosis and decrease the viability of tumor cells after 24 h of culture. These results indicate WT-VLP can enter the tumor and affect the tumor cells, so they could be used as a delivery system to the tumor. However additional studies are required to prove this possibility.

Moreover, it would be important to test the antitumoral effect in a different cancer model to establish whether the unexpected antitumoral effect of WT-VLPs seen in this model also occurs in other cancer models, as these VLPs may be used to improve tumor immunity. Although in present study we did not detect any visible signs of chronic inflammation, as manifested by skin lesions or scruffy appearance of mice. It would be also necessary to perform a complete evaluation of possible side-effects or autoimmunity induced by WT-VLPs and rMe-VLP vaccination in further studies.

Improvement in the identification and prioritization of neoepitopes and TAAs continues to be fundamental to guarantee the induction of specific responses and increase the probability of inducing strong immune responses capable of therapeutic effectiveness. Here we demonstrated that the use of neoepitopes delivered with B19-VLPs may have a therapeutic effect on tumor growth and on the establishment of macro-metastases. However, in this study we tested the potential of B19-VLPs as an antigen delivery system using a few epitopes.

Novel studies are required to further characterize the B19-VLPs as a delivery system for antigens in cancer, both with neoepitopes for cancers without known molecular targets and with recognized antigens, such as Her2, prostate-specific antigen, etc., to establish in which types of cancer the approach of VLPs with tumor antigens may be beneficial. It is also important to ascertain if these VLPs can allow the induction of humoral responses towards coupled antigens, which could extend the application of this approach to cancers where humoral responses are important.

In conclusion, we demonstrated that recombinant multiepitope-B19-VLPs could be a viable alternative as a delivery system for neoepitopes and TAAs in breast cancer, as they were able to induce specific immune responses towards the neoepitopes in lymphatic nodes near the tumor, which impacts the rate of tumor growth and the establishment of distal macro-metastasis. This approach can facilitate the application of personalized therapies, as the treatment can be delivered subcutaneously near the tumor, instead of directly in the lymph nodes. As a result, treatment administration can be performed without special ultrasound equipment. Additionally, the use of these VLPs as delivery system could avoid the processing of the antigen by non-presenting cells,

thus avoiding the induction of lymphocyte anergy and promoting the induction of powerful responses that can ultimately affect the quality of life of patients.

Declaration of Competing Interest

The authors declare that they have no known competing financial interests or personal relationships that could have appeared to influence the work reported in this paper.

Acknowledgments

This work was supported by Grants from Programa de Apoyo a Proyectos de Investigación e Innovación Tecnológica (PAPIIT) 1N2233319 and Consejo Nacional de Ciencia y Tecnología (CONACYT) CB283319. Ángel de Jesús Jiménez Chávez is a doctoral student from Programa de Doctorado en Ciencias Biomédicas, Universidad Nacional Autónoma de México (UNAM) and was supported by CONACYT (CVU 659430).

Author contributions

Conceptualization, J.C. and M.F.; Methodology, J.C.; Resources, B.J.; Investigation, J.C.; Writing – Original Draft, J.C.; Writing – Review & Editing, M.F. and B.J.: Project Administration, M.F.; Funding Acquisition, M.F.

References

[1] Bray F, Ferlay J, Soerjomataram I, Siegel RL, Torre LA, Jemal A. Global cancer statistics 2018: GLOBOCAN estimates of incidence and mortality worldwide for 36 cancers in 185 countries. CA Cancer J Clin 2018;68:394–424. https://doi.org/10.3322/caac.21492.

[2] Sahin U, Derhovanessian E, Miller M, Kloke BP, Simon P, Lower M, et al. Personalized RNA mutanome vaccines mobilize poly-specific therapeutic immunity against cancer. Nature 2017;547:222–6. https://doi.org/10.1038/nature23003.

[3] Wahba HA, El-Hadaad HA. Current approaches in treatment of triple-negative breast cancer. Cancer Biol Med 2015;12:106–16. https://doi.org/10.7497/j.issn.2095-3941.2015.0030.

[4] Brennick CA, George MM, Corwin WL, Srivastava PK, Ebrahimi-Nik H. Neoepitopes as cancer immunotherapy targets: key challenges and opportunities. Immunotherapy 2017;9:361–71. https://doi.org/10.2217/imt-2016-0146.

[5] Ott PA, Hu Z, Keskin DB, Shukla SA, Sun J, Bozym DJ, et al. An immunogenic personal neoantigen vaccine for patients with melanoma. Nature 2017;547:217–21. https://doi.org/10.1038/nature22991.

[6] Martinez-Lostao L, Anel A, Pardo J. How do cytotoxic lymphocytes kill cancer cells? Clin Cancer Res 2015;21:5047–56. https://doi.org/10.1158/1078-0432.CCR-15-0685.

[7] Marqus S, Pirogova E, Piva TJ. Evaluation of the use of therapeutic peptides for cancer treatment. J Biomed Sci 2017;24:21. https://doi.org/10.1186/s12929-017-0328-x.

[8] Yavari B, Mahjub R, Saidijam M, Raigani M, Soleimani M. The potential use of peptides in cancer treatment. Curr Protein Pept Sci 2018;19:759–70. https://doi.org/10.2174/1389203719666180111150008.

[9] Khong H, Overwijk WW. Adjuvants for peptide-based cancer vaccines. J ImmunoTher Cancer 2016;4:56. https://doi.org/10.1186/s40425-016-0160-y.

[10] Petrovsky N. Comparative safety of vaccine adjuvants: a summary of current evidence and future needs. Drug Saf 2015;38:1059–74. https://doi.org/10.1007/s40264-015-0350-4.

[11] Abraham M, Karni A, Dembinsky A, Miller A, Gandhi R, Anderson D, et al. In vitro induction of regulatory T cells by anti-CD3 antibody in humans. J Autoimmun 2008;30:21–8. https://doi.org/10.1016/j.jaut.2007.11.007.

[12] Chen L, Flies DB. Molecular mechanisms of T cell co-stimulation and co-inhibition. Nat Rev Immunol 2013;13:227–42. https://doi.org/10.1038/nri3405.

[13] Zdanowicz M, Chroboczek J. Virus-like particles as drug delivery vectors. Acta Biochim Pol 2016;63:469–73. https://doi.org/10.18388/abp.2016_1275.

[14] Ong HK, Tan WS, Ho KL. Virus like particles as a platform for cancer vaccine development. PeerJ 2017;5:e4053. https://doi.org/10.7717/peerj.4053.

[15] Palladini A, Thrane S, Janitzek CM, Pihl J, Clemmensen SB, de Jongh WA, et al. Virus-like particle display of HER2 induces potent anti-cancer responses. Oncoimmunology 2018;7:e1408749. https://doi.org/10.1080/2162402X.2017.1408749.

[16] Lin MC, Wang M, Chou MC, Chao CN, Fang CY, Chen PL, et al. Gene therapy for castration-resistant prostate cancer cells using JC polyomavirus-like particles packaged with a PSA promoter driven-suicide gene. Cancer Gene Ther 2019. https://doi.org/10.1038/s41417-019-0083-0.

[17] Ao Z, Chen W, Tan J, Cheng Y, Xu Y, Wang L, et al. Lentivirus-based virus-like particles mediate delivery of caspase 8 into breast cancer cells and inhibit tumor growth. Cancer Biother Radiopharm 2019;34:33–41. https://doi.org/10.1089/cbr.2018.2566.

[18] Jia C, Yang T, Liu Y, Zhu A, Yin F, Wang Y, et al. A novel human papillomavirus 16 L1 pentamer-loaded hybrid particles vaccine system: influence of size on immune responses. ACS Appl Mater Interfaces 2018. https://doi.org/10.1021/acsami.8b11556.

[19] Sanchez-Rodriguez SP, Munch-Anguiano L, Echeverria O, Vazquez-Nin G, Mora-Pale M, Dordick JS, et al. Human parvovirus B19 virus-like particles: In vitro assembly and stability. Biochimie 2012;94:870–8. https://doi.org/10.1016/j.biochi.2011.12.006.

[20] Bustos-Jaimes I, Soto-Roman RA, Gutierrez-Landa IA, Valadez-Garcia J, Segovia-Trinidad CL. Construction of protein-functionalized virus-like particles of parvovirus B19. J Biotechnol 2017;263:55–63. https://doi.org/10.1016/j.jbiotec.2017.09.014.

[21] Moron G, Rueda P, Casal I, Leclerc C. CD8alpha- CD11b+ dendritic cells present exogenous virus-like particles to CD8+ T cells and subsequently express CD8alpha and CD205 molecules. J Exp Med 2002;195:1233–45. https://doi.org/10.1084/jem.20011930.

[22] Kreiter S, Vormehr M, van de Roemer N, Diken M, Lower M, Diekmann J, et al. Mutant MHC class II epitopes drive therapeutic immune responses to cancer. Nature 2015;520:692–6. https://doi.org/10.1038/nature14426.

[23] Kim K, Skora AD, Li Z, Liu Q, Tam AJ, Blosser RL, et al. Eradication of metastatic mouse cancers resistant to immune checkpoint blockade by suppression of myeloid-derived cells. PNAS 2014;111:11774–9. https://doi.org/10.1073/pnas.1410626111.

[24] Jaiswal PK, Goel A, Mittal RD. Survivin: A molecular biomarker in cancer. Ind J Med Res 2015;141:389–97. https://doi.org/10.4103/0971-5916.159250.

[25] Amexis G, Young NS. Parvovirus B19 empty capsids as antigen carriers for presentation of antigenic determinants of dengue 2 virus. J Infect Dis 2006;194:790–4. https://doi.org/10.1086/506361.

[26] Ogasawara Y, Amexis G, Yamaguchi H, Kajigaya S, Leppla SH, Young NS. Recombinant viral-like particles of parvovirus B19 as antigen carriers of anthrax protective antigen. vivo 2006;20:319–24.

[27] Gilbert L, Toivola J, White D, Ihalainen T, Smith W, Lindholm L, et al. Molecular and structural characterization of fluorescent human parvovirus B19 virus-like particles. Biochem Biophys Res Commun 2005;331:527–35. https://doi.org/10.1016/j.bbrc.2005.03.208.

[28] Gonzalez-Gonzalez E, Garcia-Hernandez AL, Flores-Mejia R, Lopez-Santiago R, Moreno-Fierros L. The protoxin Cry1Ac of Bacillus thuringiensis improves the protection conferred by intranasal immunization with Brucella abortus RB51 in a mouse model. Vet Microbiol 2015;175:382–8. https://doi.org/10.1016/j.vetmic.2014.11.021.

[29] Moreno-Fierros L, Garcia-Hernandez AL, Ilhuicatzi-Alvarado D, Rivera-Santiago L, Torres-Martinez M, Rubio-Infante N, et al. Cry1Ac protoxin from Bacillus thuringiensis promotes macrophage activation by upregulating CD80 and CD86 and by inducing IL-6, MCP-1 and TNF-alpha cytokines. Int Immunopharmacol 2013;17:1051–66. https://doi.org/10.1016/j.intimp.2013.10.005.

[30] Zimmerman T, Petit Frere C, Satzger M, Raba M, Weisbach M, Dohn K, et al. Simultaneous metal chelate affinity purification and endotoxin clearance of recombinant antibody fragments. J Immunol Methods 2006;314:67–73. https://doi.org/10.1016/j.jim.2006.05.012.

[31] Pulaski BA, Ostrand-Rosenberg S. Mouse 4T1 breast tumor model. Curr Prot Immunol 2001. https://doi.org/10.1002/0471142735.im2002s39. Chapter 20: Unit 20 2.

[32] Rojas-Hernandez S, Rodriguez-Monroy MA, Lopez-Revilla R, Resendiz-Albor AA, Moreno-Fierros L. Intranasal coadministration of the Cry1Ac protoxin with amoebal lysates increases protection against Naegleria fowleri meningoencephalitis. Infect Immun 2004;72:4368–75. https://doi.org/10.1128/IAI.72.8.4368-4375.2004.

[33] Li Z, Pang Y, Gara SK, Achyut BR, Heger C, Goldsmith PK, et al. Gr-1+CD11b+ cells are responsible for tumor promoting effect of TGF-beta in breast cancer progression. Int J Cancer 2012;131:2584–95. https://doi.org/10.1002/ijc.27572.

[34] Tsubaki T, Kadonosono T, Sakurai S, Shiozawa T, Goto T, Sakai S, et al. Novel adherent CD11b(+) Gr-1(+) tumor-infiltrating cells initiate an immunosuppressive tumor microenvironment. Oncotarget 2018;9:11209–26. https://doi.org/10.18632/oncotarget.24359.

[35] Gregorio AC, Fonseca NA, Moura V, Lacerda M, Figueiredo P, Simoes S, et al. Inoculated cell density as a determinant factor of the growth dynamics and metastatic efficiency of a breast cancer murine model. PLoS ONE 2016;11:e0165817. https://doi.org/10.1371/journal.pone.0165817.

[36] Manolova V, Flace A, Bauer M, Schwarz K, Saudan P, Bachmann MF. Nanoparticles target distinct dendritic cell populations according to their size. Eur J Immunol 2008;38:1404–13. https://doi.org/10.1002/eji.200737984.

[37] Li K, Peers-Adams A, Win SJ, Scullion S, Wilson M, Young VL, et al. Antigen incorporated in virus-like particles is delivered to specific dendritic cell subsets that induce an effective antitumor immune response in vivo. J Immunother 2013;36:11–9. https://doi.org/10.1097/CJI.0b013e3182787f5e.

[38] Peacey M, Wilson S, Perret R, Ronchese F, Ward VK, Young V, et al. Virus-like particles from rabbit hemorrhagic disease virus can induce an anti-tumor response. Vaccine 2008;26:5334–7. https://doi.org/10.1016/j.vaccine.2008.07.074.

[39] Tomita Y, Nishimura Y. Long peptide-based cancer immunotherapy targeting tumor antigen-specific CD4(+) and CD8(+) T cells. Oncoimmunology 2013;2: e25801. https://doi.org/10.4161/onci.25801.
[40] Zanetti M. Tapping CD4 T cells for cancer immunotherapy: the choice of personalized genomics. J Immunol 2015;194:2049–56. https://doi.org/10.4049/jimmunol.1402669.
[41] Rahman M, Mohammed S. Breast cancer metastasis and the lymphatic system. Oncol Lett 2015;10:1233–9. https://doi.org/10.3892/ol.2015.3486.
[42] Blackburn HL, Ellsworth DL, Shriver CD, Ellsworth RE. Breast cancer metastasis to the axillary lymph nodes: are changes to the lymph node "Soil" localized or systemic? Breast Canc Basic Clin Res 2017;11:1. https://doi.org/10.1177/1178223417691246. 1178223417691246.
[43] Zheng K, Li Q, Fu C, Ma S. Inhibitory effects of 4T1 breast tumor transplantation on mouse peripheral blood immune cell populations. Biotechnol J Int 2017;19:1–12. https://doi.org/10.9734/BJI/2017/36382.
[44] Youn JI, Nagaraj S, Collazo M, Gabrilovich DI. Subsets of myeloid-derived suppressor cells in tumor-bearing mice. J Immunol 2008;181:5791–802. https://doi.org/10.4049/jimmunol.181.8.5791.
[45] Umansky V, Blattner C, Gebhardt C, Utikal J. The role of myeloid-derived suppressor cells (MDSC) in cancer progression. Vaccines 2016;4. https://doi.org/10.3390/vaccines4040036.
[46] Shirota H, Tross D, Klinman DM. CpG oligonucleotides as cancer vaccine adjuvants. Vaccines 2015;3:390–407. https://doi.org/10.3390/vaccines3020390.
[47] Brown KE, Anderson SM, Young NS. Erythrocyte P antigen: cellular receptor for B19 parvovirus. Science 1993;262:114–7. https://doi.org/10.1126/science.8211117.
[48] Weigel-Kelley KA, Yoder MC, Srivastava A. Alpha5beta1 integrin as a cellular coreceptor for human parvovirus B19: requirement of functional activation of beta1 integrin for viral entry. Blood 2003;102:3927–33. https://doi.org/10.1182/blood-2003-05-1522.
[49] Seung-Yeol P, Chan-Yeong K, James AS, Jung HK. Globoside (Gb4) promotes activation of ERK by interaction with the epidermal growth factor receptor. BBA 2012;1820:1141–8. https://doi.org/10.1016/j.bbagen.2012.04.008.
[50] Roman J, Ritzenthaler JD, Roser-Page S, Xiaojuan S, ShouWei H. α5β1-integrin expression is essential for tumor progression in experimental lung cancer. Am J Respir Cell Mol Biol 2010;43:684–91. https://doi.org/10.1165/rcmb.2009-0375OC.
[51] Mierke CT, Frey B, Fellner M, Hermann M, Fabry B. Integrin α5β1 facilitates cancer cell invasion through enhanced contractile forces. J Cell Sci 2011;124:369–83. https://doi.org/10.1242/jcs.071985.